Am J Physiol Heart Circ Physiol 309: H2058–H2066, 2015.
First published October 9, 2015; doi:10.1152/ajpheart.00376.2015.

An intact small animal model of myocardial ischemia-reperfusion: Characterization of metabolic changes by hyperpolarized ^{13}C MR spectroscopy

Hikari A. I. Yoshihara,[1,4,5] Jessica A. M. Bastiaansen,[3,4] Corinne Berthonneche,[2] Arnaud Comment,[3,4] and Juerg Schwitter[1,5]

[1]*Division of Cardiology, Lausanne University Hospital (CHUV), Lausanne, Switzerland;* [2]*Cardiovascular Assessment Facility, Lausanne University Hospital (CHUV), Lausanne, Switzerland;* [3]*Institute of Physics of Biological Systems, Swiss Federal Institute of Technology (EPFL), Lausanne, Switzerland;* [4]*Center for Biomedical Imaging (CIBM), Lausanne, Switzerland;* [5]*Cardiac MR Center, Lausanne University Hospital (CHUV), Lausanne, Switzerland*

Submitted 19 May 2015; accepted in final form 8 October 2015

Yoshihara HA, Bastiaansen JA, Berthonneche C, Comment A, Schwitter J. An intact small animal model of myocardial ischemia-reperfusion: Characterization of metabolic changes by hyperpolarized ^{13}C MR spectroscopy. *Am J Physiol Heart Circ Physiol* 309: H2058–H2066, 2015. First published October 9, 2015; doi:10.1152/ajpheart.00376.2015.—Hyperpolarized carbon-13 magnetic resonance spectroscopy (^{13}C MRS) enables the sensitive and noninvasive assessment of the metabolic changes occurring during myocardial ischemia-reperfusion. Ischemia-reperfusion models using hyperpolarized ^{13}C MRS are established in heart preparations ex vivo and in large animals in vivo, but an in vivo model in small animals would be advantageous to allow the study of reperfusion metabolism with neuroendocrine and inflammatory responses intact with the option to perform a greater number of experiments. A novel intact rat model of ischemia-reperfusion is presented that incorporates hyperpolarized ^{13}C MRS to characterize reperfusion metabolism. Typically, in an in vivo model, a tissue input function (TIF) is required to account for apparent changes in the metabolism of injected hyperpolarized [1-^{13}C]pyruvate resulting from changes in perfusion. Whereas the measurement of a TIF by metabolic imaging is particularly challenging in small animals, the ratios of downstream metabolites can be used as an alternative. The ratio of [^{13}C]bicarbonate:[1-^{13}C]lactate ($Ratio_{Bic/Lac}$) measured within 1–2 min after coronary release decreased vs. baseline in ischemic rats ($n = 10$, 15-min occlusion, controls: $n = 10$; $P = 0.017$ for interaction, 2-way ANOVA). The decrease in oxidative pyruvate metabolism [$Ratio_{Bic/Lac(Ischemia)}$/$Ratio_{Bic/Lac(Baseline)}$] modestly correlated with area at risk ($r = 0.66$; $P = 0.002$). Hyperpolarized ^{13}C MRS was also used to examine alanine production during ischemia, which is observed in ex vivo models, but no significant change was noted; metrics incorporating [1-^{13}C]alanine did not substantially improve the discrimination of ischemic-reperfused myocardium from nonischemic myocardium. This intact rat model, which mimics the human situation of reperfused myocardial infarction, could be highly valuable for the testing of new drugs to treat reperfusion injury, thereby facilitating translational research.

hyperpolarization; heart; dynamic nuclear polarization; magnetic resonance spectroscopy; carbon-13

NEW & NOTEWORTHY

For the first time in an intact rat model, hyperpolarized ^{13}C spectroscopy is used to follow changes in myocardial energy metabolism in ischemia-reperfusion. This model can explore ischemia-reperfusion metabolism with preserved neuro-endocrine and inflammatory responses, and in translational research it can test novel treatment strategies in acute reperfused myocardial infarction.

CARDIOVASCULAR DISEASES REMAIN a leading cause of death in the industrialized world (1). Of these, the most prevalent is coronary artery disease, which can cause acute restriction of blood supply to the myocardium. In the setting of acute myocardial infarction (AMI), the most successful treatment today is to revascularize the tissue within hours to stop ongoing necrosis (34, 44). However, the so-called reperfusion injury itself adds additional tissue damage to the infarct region (46). Several strategies have been tested to mitigate this reperfusion damage in large clinical trials with varying success (5, 6, 42). Hyperpolarized ^{13}C magnetic resonance spectroscopy and imaging techniques (MRS and MRI) (2, 20, 21) offer the unique possibility to assess noninvasively metabolic changes in the myocardium during ischemia and reperfusion. A better understanding of metabolic alterations occurring during ischemia-reperfusion would aid the design of new treatment strategies in patients with AMI undergoing acute revascularizations. To develop such strategies and to test their efficacy, animal models incorporating hyperpolarized ^{13}C-magnetic resonance are highly desirable. Such models should test metabolic changes immediately and noninvasively upon reperfusion and should be established in small animals. It is crucial to probe ischemia-reperfusion metabolism in an intact animal, as that allows one to assess metabolism and test therapeutic metabolic interventions while other important mechanisms such as neuroendocrine activation and reactive inflammation remain active. Thus an intact animal better models AMI in humans and represents an important complement to models based on isolated heart preparations in facilitating translational research. In addition, it is desirable to establish such an intact model in a small animal to address questions with a sufficient number of experiments while keeping costs at a reasonable level. Currently, in models of myocardial ischemia-reperfusion, hyperpolarized ^{13}C MRS and MRI are implemented in either ex vivo preparations of small animal hearts (10, 28, 38, 41) or in intact large animal models (3, 4, 21, 25). The aims of this study were twofold, first, to develop an intact small animal model that uses hyperpolarized ^{13}C MRS, and second, to characterize its metabolism during ischemia-reperfusion, examining the changes in bicar-

Address for reprint requests and other correspondence: J. Schwitter, Div. of Cardiology and CMR Center, Rue du Bugnon 46, CH-1011 Lausanne, Switzerland (e-mail: jurg.schwitter@chuv.ch).

bonate, lactate, and alanine production from pyruvate injected during reperfusion.

The application of hyperpolarized ^{13}C MRS in a small intact animal model faces a major challenge. Whereas metabolic studies in chronic heart diseases can be performed under the assumption that tissue perfusion remains stable during the experiments (8, 17, 18, 39, 40, 43), substantial changes in perfusion are anticipated in the setting of ischemia-reperfusion. Therefore, a tissue input function (TIF) is required to take into account changes in metabolite signals resulting from changes in the myocardial delivery of the ^{13}C-labeled substrate, and not from tissue metabolic changes per se. This is not an issue with global ischemia in ex vivo perfused heart preparations, as the delivery of substrates is uniform and controllable (28, 38, 41). On the other hand, the TIF can be derived by an imaging approach in an intact large animal model; however, the benefit is not clear, as the TIF for hyperpolarized [1-^{13}C]pyruvate could not improve the calculation of fluxes to [^{13}C]bicarbonate and [1-^{13}C]lactate (25). The measurement of the TIF might be even more challenging in small animal hearts, which require higher-resolution imaging, limiting reproducibility and requiring larger sample sizes. Therefore, we decided to test the hypothesis that the ratio of metabolites can be used as an indicator of metabolic changes without the need to measure a TIF. This strategy was already explored in ex vivo small heart preparations, and the [^{13}C]bicarbonate:[1-^{13}C]lactate ratio is sensitive to metabolic changes during ischemia-reperfusion, as reported by Merritt et al. (28) and others (9).

Some studies in perfused isolated hearts report an increase in alanine production during ischemia, likely resulting from increased anaplerosis (15, 36, 37). Because hyperpolarized [1-^{13}C]pyruvate probes the alanine pool size via its reversible conversion with alanine aminotransferase, we therefore addressed a second question with this study, whether the additional quantification of alanine production during ischemia-reperfusion allows for a better discrimination of ischemic-reperfused myocardium from normal healthy myocardium in the presented intact small animal model.

MATERIALS AND METHODS

Materials. [1-^{13}C]pyruvic acid and deuterium oxide were purchased from Sigma-Aldrich (Buchs, Switzerland). Formulations of [1-^{13}C]pyruvic acid with trityl radical OX063 (tris(8-carboxy-2,2,6,6-tetrakis(2-hydroxyethyl)benzo[1,2-*d*:4,5-*d′*]bis([1,3]dithiole)-4-yl)methyl sodium salt) were prepared by Albeda Research (Copenhagen, Denmark).

Animals. Experiments involving animals were performed in accordance with local and federal regulations (Swiss Federal Act on Animal Protection) and were authorized by the Service de la consommation et des affaires vétérinaires (SCAV - EXPANIM) of the Canton of Vaud, Switzerland. Male Wistar rats (n = 34; 267.1 ± 18.5 g) (mean ± SD) were obtained from Charles River (Châtillon-sur-Chalaronne, France). Experiments were started and performed at the same time of day to control for any potential metabolic differences related to the circadian rhythm.

Experimental protocol. Before surgery, rats were anaesthetized with isoflurane (5%), intubated, and mechanically ventilated (MRI-1; CWE, Ardmore, PA) with air, 50% oxygen, and 2% isoflurane. Both femoral arteries were catheterized to allow blood sampling and monitoring of blood pressure and heart rate. One femoral vein was catheterized for infusions. A left thoracotomy was performed, and the fourth intercostal space was entered to access the heart. A 5.0 suture thread was passed under the left coronary artery (LCA) 3–8 mm from the tip of the left auricle. The ends of the thread were passed through a short piece of polyethylene tubing with flared ends, forming a loose snare around the LCA. Rats in both the ischemia group and the control group underwent the same surgery to install the occluding thread. The thoracotomy was stitched up, leaving the ends of the thread and tube protruding. The rat was placed supine in a holder tray, and a surface coil with a single 16-mm loop for ^{1}H and two 16-mm loops for ^{13}C in quadrature was placed over the heart. A rectal temperature probe, pneumatic respiration sensor, and blood pressure sensor (Small Animal Instruments, Stony Brook, NY) were installed for physiological monitoring. Heating was provided by warm water circulating through tubing placed next to the rat. Before loading the rat into the scanner, 0.2 mg/kg of pancuronium bromide was administered intravenously to suppress any spontaneous breathing motion of the diaphragm, facilitating reliable acquisition gating and shimming.

Hemodynamic monitoring. The rate of respiration was maintained between 60 and 70 breaths/min, and body temperature kept between 37.5 and 38.5°C. Blood samples were taken periodically throughout the experiment to monitor P_{CO_2}, O_2 saturation, and pH, and normal levels were maintained by adjusting ventilation rate, tidal volume, and O_2 content. Additionally, blood lactate was measured before the baseline [1-^{13}C]pyruvate infusion, before the period of ischemia, and after 10 min of ischemia.

Polarization. Neat [1-^{13}C]pyruvic acid containing 21 mM OX063 (17 μl) was transferred to a polytetrafluoroethylene sample cup and frozen using liquid nitrogen. A stoichiometric equivalent of 10 M NaOH for neutralization was added to the cup and frozen separately. The pyruvic acid sample was negatively polarized at 7 T and 1.0 K with microwave irradiation at 196.80 GHz in a custom-built dissolution-dynamic nuclear polarization polarizer (13), then dissolved with 6 ml of D_2O containing 47 mM sodium phosphate, 100 mM NaCl, 2.7 mM KCl, 0.3 mM EDTA, pH 7.4, and rapidly transferred to a remote-controlled phase separator/infusion pump yielding a polarization of 45–55% (14, 16).

Anatomic imaging and hyperpolarized ^{13}C spectroscopy. MRI and MRS were performed in a 9.4-T, 31-cm horizontal bore magnet (Magnex Scientific, Oxford, UK) with a VNMRS console (Varian, Palo Alto, CA). Gradient echo ^{1}H imaging was used to ensure the correct placement of the coil over the heart and to localize the voxel used for shimming and localized spectroscopy. Shimming was performed using the FAST(EST)MAP gradient shimming routine (22) with a voxel placed above and including the ventral side of the left ventricle (LV), to a water line width of 35–50 Hz by stimulated echo localized spectroscopy using the same voxel. The metabolism of infused hyperpolarized [1-^{13}C]pyruvate (at a dose of 0.3 mmol/kg in 1.8 ml) was monitored by ^{13}C MRS. The acquisition of a series of 40 respiration and cardiac-gated spectra (30° BIR-4 adiabatic pulse, transmitter at ~175 ppm, spectral width: 20,161 Hz, acquisition time: 205 ms, WALTZ-16 ^{1}H decoupling, repetition time ~3 s) was started at the beginning of the infusion. After the second infusion, late gadolinium enhancement (LGE) was performed with 0.12 mmol/kg gadoteridol administered intravenously and T_1-weighted inversion-recovery gradient echo imaging performed 20 min later (12).

Baseline and postischemia metabolism. An infusion of hyperpolarized [1-^{13}C]pyruvate was performed after shimming to establish the baseline metabolic state of the heart (Fig. 1). Another polarization was started immediately following this first hyperpolarized [1-^{13}C]pyruvate infusion. After 90–120 min, myocardial ischemia was induced. Another dose of pancuronium bromide (0.1 mg/kg) was infused to ensure regular breathing and proper acquisition gating. With the rat outside the scanner bore, but still positioned in the holder, the LCA was occluded by tightening the occluding suture thread and clamping it in place against the polyethylene tubing using a titanium clip. In control experiments, the thread was not tightened. After 15 min, the occlusion was released. This occlusion time was chosen to minimize the risk of inducing necrosis. The rat was then returned immediately to its prior position in the scanner, and the second infusion of

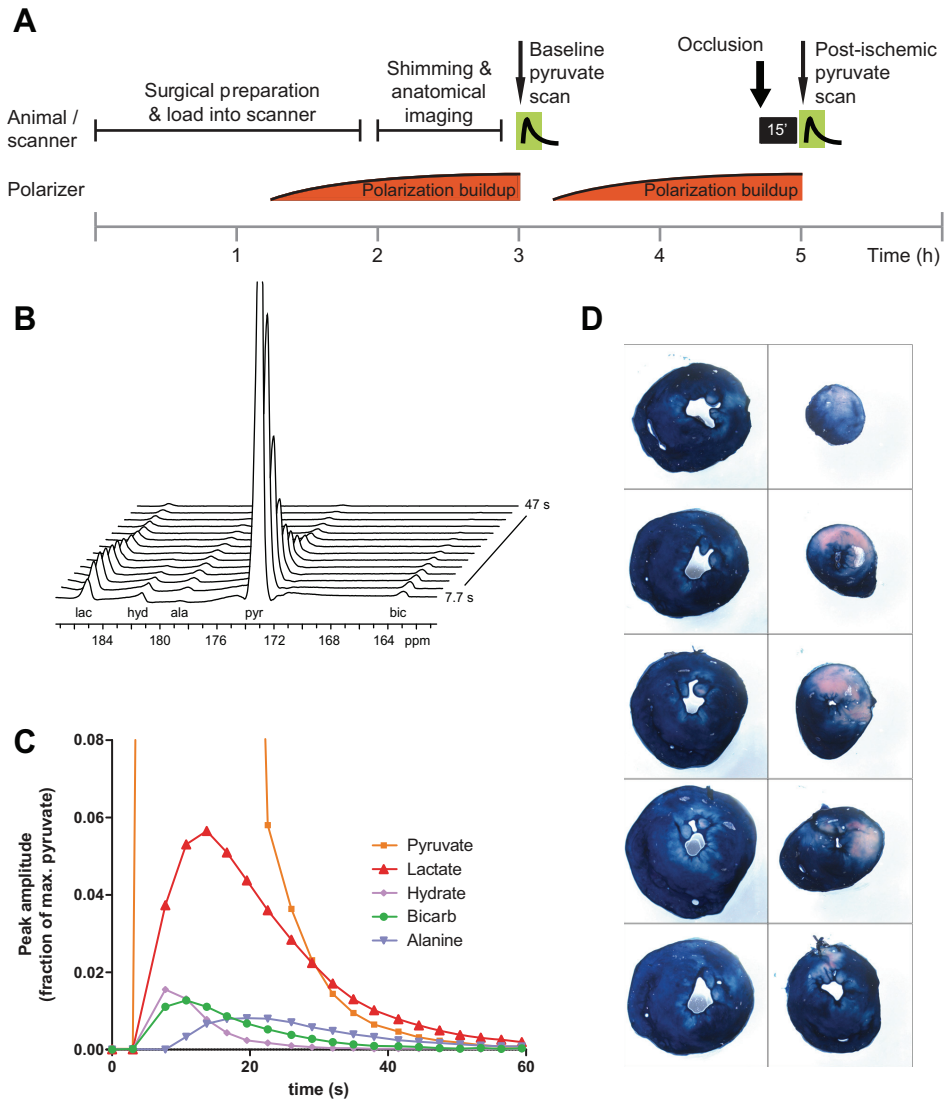

Fig. 1. *A*: timeline of hyperpolarized myocardial ischemia-reperfusion experiment. After preparation, shimming, and positioning, hyperpolarized [1-^{13}C]pyruvate was infused to establish baseline metabolism. Myocardial metabolism during early reperfusion was assessed by a hyperpolarized infusion immediately following 15 min of left carotid artery occlusion. The occlusion was omitted in control experiments. *B*: typical time course of ^{13}C magnetic resonance spectroscopy spectra of heart metabolism of infused polarized [1-^{13}C]pyruvate. Stacked spectra acquired at ~3-s intervals show evolution of metabolite signals [1-^{13}C]lactate (lac, 185.0 ppm), [^{13}C]bicarbonate (bic, 162.8 ppm), and [1-^{13}C]alanine (ala, 178.4 ppm), as well as signal decay of infused [1-^{13}C]pyruvate (pyr, 172.9 ppm) and its hydrated form (hyd, 181.2 ppm). *C*: evolution of metabolite signals over time, scaled to fraction of maximum pyruvate signal. *D*: example of Evans blue-stained heart slices (1 mm thick). Occluding thread was tightened before injecting stain, and the moderate area at risk appears unstained in the apical region of the heart.

hyperpolarized [1-^{13}C]pyruvate was performed without delay, i.e., 75–120 s after occlusion release. This short interval was chosen because the largest changes in lactate and bicarbonate production occur immediately after reperfusion studied in isolated rat hearts (28), and these events normalize upon further reperfusion.

Upon completion of scanning, the rats were removed from the magnet and euthanized with pentobarbital sodium (100 mg/kg). The heart was immediately removed, rinsed with PBS, and perfused with Evans Blue after tying the occluding thread tight. The stained heart was then rinsed, cut into 1-mm-thick axial slices, and photographed. Unstained areas were calculated from the images of the slices using ImageJ (U. S. National Institutes of Health, Bethesda, MD). The area at risk was expressed as a percentage of total ventricular surface. An example is given in Fig. 1*D*.

Data analysis. Data sets with irregularly shaped or broad spectral peaks >80 Hz wide at half maximum were excluded (controls: 2; ischemia group: 2) due to difficulties with their accurate quantitation, as were incomplete experiments (control group: 1; ischemia group: 2). Experiments with physiological irregularities were also excluded, specifically those in which blood lactic acid levels exceeded 45 mg/dl and pH was below 7.35 (control group: 3; ischemia group: 2), indicating lactic acidosis (26); those in which blood glucose levels differed by more than two standard deviations from the mean (controls: 1), or those in which the systolic blood pressure did not partially recover after LCA occlusion (ischemia group: 1). Spectral peaks were quantified by FID fitting using Bayes (Washington University, St. Louis, MO) and visually inspected for goodness of fit. The area under the curve (AUC) for each metabolite was calculated using the fitted peak area and the time interval between each respiration and cardiac gated spectral acquisition. The following metabolite ratios were calculated from the AUC values: $\text{Ratio}_{\text{Bic/Lac}} = \text{AUC}_{\text{Bic}}/\text{AUC}_{\text{Lac}}$; $\text{Ratio}_{\text{Bic/Lac+Ala}} = \text{AUC}_{\text{Bic}}/(\text{AUC}_{\text{Lac}} + \text{AUC}_{\text{Ala}})$; $\text{Ratio}_{\text{Bic/Ala}} = \text{AUC}_{\text{Bic}}/\text{AUC}_{\text{Ala}}$; $\text{Ratio}_{\text{Lac/Ala}} = \text{AUC}_{\text{Lac}}/\text{AUC}_{\text{Ala}}$; $\text{Ratio}_{\text{Base}}$ = $\text{Ratio}_{\text{Bic/Lac}}$, $\text{Ratio}_{\text{Bic/Ala}}$, $\text{Ratio}_{\text{Lac/Ala}}$, or $\text{Ratio}_{\text{Bic/Lac+Ala}}$ measured at baseline; $\text{Ratio}_{\text{Isch}}$ = $\text{Ratio}_{\text{Bic/Lac}}$, $\text{Ratio}_{\text{Bic/Ala}}$, $\text{Ratio}_{\text{Lac/Ala}}$, or $\text{Ratio}_{\text{Bic/Lac+Ala}}$ measured upon reperfusion; $\text{Ratio}_{\text{Metabolite/total signal}} = \text{AUC}_{\text{Metabolite}}/(\text{AUC}_{\text{Lac}} + \text{AUC}_{\text{Hydrate}} + \text{AUC}_{\text{Ala}} + \text{AUC}_{\text{Pyr}} + \text{AUC}_{\text{Bic}})$.

Statistics. Results are reported as means ± SE. Statistical and linear regression analyses were performed using GraphPad Prism (v. 5.04; GraphPad Software, La Jolla, CA). The influence of intervention (ischemia-reperfusion vs. sham) on the change of $\text{Ratio}_{\text{Base}}$ and $\text{Ratio}_{\text{Isch}}$ was assessed by using a two-way ANOVA for repeated measures. The influence of intervention (ischemia-reperfusion vs. sham) on the change in $\text{Ratio}_{\text{Isch}}/\text{Ratio}_{\text{Base}}$ was assessed by using a two-tailed Student's *t*-test. A P value <0.05 was considered statistically significant.

Table 1. *Summary of animal physiological parameters for rats in control and ischemia groups*

Parameter	Control	Ischemia
n	10	10
Heart rate, beats/min	420 ± 6	454 ± 8
Body weight, g	269.3 ± 6.3	264.3 ± 3.4
Body temperature, °C	37.5 ± 0.1	37.9 ± 0.1
Blood lactic acid, mg/dl	20.6 ± 1.1	22.4 ± 1.0
Blood glucose, mg/dl	171.6 ± 7.3	157.1 ± 8.0
Δ Systolic BP upon occlusion, mmHg	—	−34.8 ± 5.5
Δ Diastolic BP upon occlusion, mmHg	—	−13.1 ± 3.8

Values are means ± SE. BP, blood pressure.

RESULTS

The hyperpolarized metabolites [1-^{13}C]lactate, [1-^{13}C]alanine, and [^{13}C]bicarbonate were detected within seconds after the infusion of hyperpolarized [1-^{13}C]pyruvate, with lactate being the predominant metabolite signal (Fig. 1, *B* and *C*). Occlusion of the LCA to create an ischemic area in the LV myocardium was accompanied by a drop in both systolic and diastolic blood pressure (−34.8 ± 5.5 and −13.1 ± 3.8 mmHg, respectively; Table 1), which partially recovered over several minutes. The set of completed experiments with good spectral data and without lactic acidosis consisted of 10 controls and 10 ischemic rats. Controls were "sham-occluded" in that they underwent the same preparation and experimental protocol, except that the occluding thread was not tightened.

$Ratio_{Bic/Lac}$ to detect ischemic metabolism. The ratio of hyperpolarized [^{13}C]bicarbonate to [1-^{13}C]lactate ($Ratio_{Bic/Lac}$), an indicator of oxidative pyruvate metabolism of the myocardium, decreased from baseline ($Ratio_{Base}$) to ischemia-reperfusion ($Ratio_{Isch}$) in the ischemia group ($n = 10$), but not in the controls ($n = 10$; $P = 0.017$ for the interaction Ratio-intervention, 2-way ANOVA for repeated measures) as shown in Fig. 2. Using $Ratio_{Bic/Lac}$, a decrease of $Ratio_{Isch}/Ratio_{Base}$ indicates a shift toward anaerobic metabolism as shown in Fig. 3. $Ratio_{Isch}/Ratio_{Base}$ was lower in the ischemic group than in the control group (0.74 ± 0.06 vs. 1.16 ± 0.10 in controls, $P = 0.002$, Fig. 3*A*).

The size of the area at risk, determined by Evans Blue staining (Fig. 1*D*) in 9 of the 10 experiments with ischemia, ranged from mild to severe (4.4–47.5% of the LV, respectively) with a mean of 28.6 ± 4.7%. Plotting $Ratio_{Isch}/Ratio_{Base}$ against the area at risk shows a clear trend toward a greater metabolic change with a larger area at risk (Fig. 3*C*). Linear regression analysis including the control experiments with zero area at risk yields a negative slope, indicating a greater decrease in $Ratio_{Isch}/Ratio_{Base}$ with larger area at risk. The regression line intersects the *y*-axis at 1.11 ± 0.08, consistent with no change or a slight improvement in $Ratio_{Bic/Lac}$ in animals with no area at risk. With only two points between 0 and 20% area at risk, the correlation is no longer significant ($P = 0.18$) with the control points excluded.

With a 15-min period of occlusion followed shortly by LGE MRI, the area at risk was expected to remain viable, and necrosis was not anticipated. However, tissue damage resulting from the surgery 5 h earlier could result in necrosis. LGE was negative in all surviving cases, indicating that little if any necrotic myocardium resulted from the surgical preparation and experimental procedure. As it was not possible to perform LGE in the animals dying during the experiments ($n = 2$), necrosis in these animals cannot be excluded.

[1-^{13}C]alanine production. As there is evidence that alanine is produced by the ischemic myocardium through anaplerotic pathways, the ratio of bicarbonate to lactate plus alanine ($Ratio_{Bic/Lac+Ala}$) was also evaluated. Examining the change in $Ratio_{Bic/Lac+Ala}$ between baseline and ischemia conditions, we found a *P* value for the interaction of intervention-ratio of 0.015 (Fig. 2*B*, 2-way ANOVA for repeated measures), indicating that taking the alanine signal into account marginally improved the ability to detect ischemic myocardium, as using $Ratio_{Bic/Lac}$ yielded a *P* Value for interaction of 0.017. Conversely, the difference in $Ratio_{Isch}/Ratio_{Base}$ calculated using $Ratio_{Bic/Lac+Ala}$ (0.76 ± 0.07 vs. 1.15 ± 0.07 in controls, $P = 0.001$, Fig. 3*B*) closely resembles the result using $Ratio_{Bic/Lac}$.

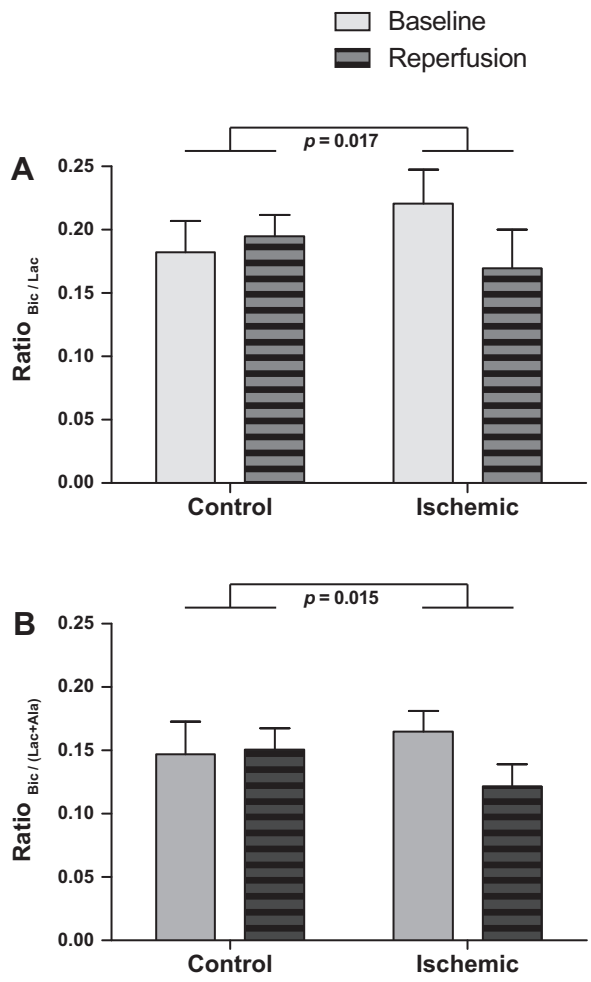

Fig. 2. *A*: ratio of hyperpolarized [^{13}C]bicarbonate to [1-^{13}C]lactate ($Ratio_{Bic/Lac}$) is shown as a measure of oxidative pyruvate metabolism of the myocardium for the ischemia and control groups at baseline (shaded bars) and ischemia-reperfusion (hashed bars). A decreasing ratio indicates less pyruvate oxidation or more lactate production and a shift toward anaerobic metabolism. The ratio is independent of the tissue input function, as both metabolites originate from the same substrate. In controls, $Ratio_{Bic/Lac}$ did not change between baseline and ischemia-reperfusion measurements, whereas it decreased in the ischemic groups ($P = 0.017$ for the interaction of ratio intervention, 2-way ANOVA for repeated measures). *B*: ratio of hyperpolarized [^{13}C]bicarbonate to the sum of [1-^{13}C]lactate and [1-^{13}C]alanine ($Ratio_{Bic/Lac+Ala}$) at baseline (shaded bars) and ischemia-reperfusion (hashed bars). For $Ratio_{Bic/Lac+Ala}$ the *P* value for interaction of ratio intervention is 0.015 (2-way ANOVA for repeated measures).

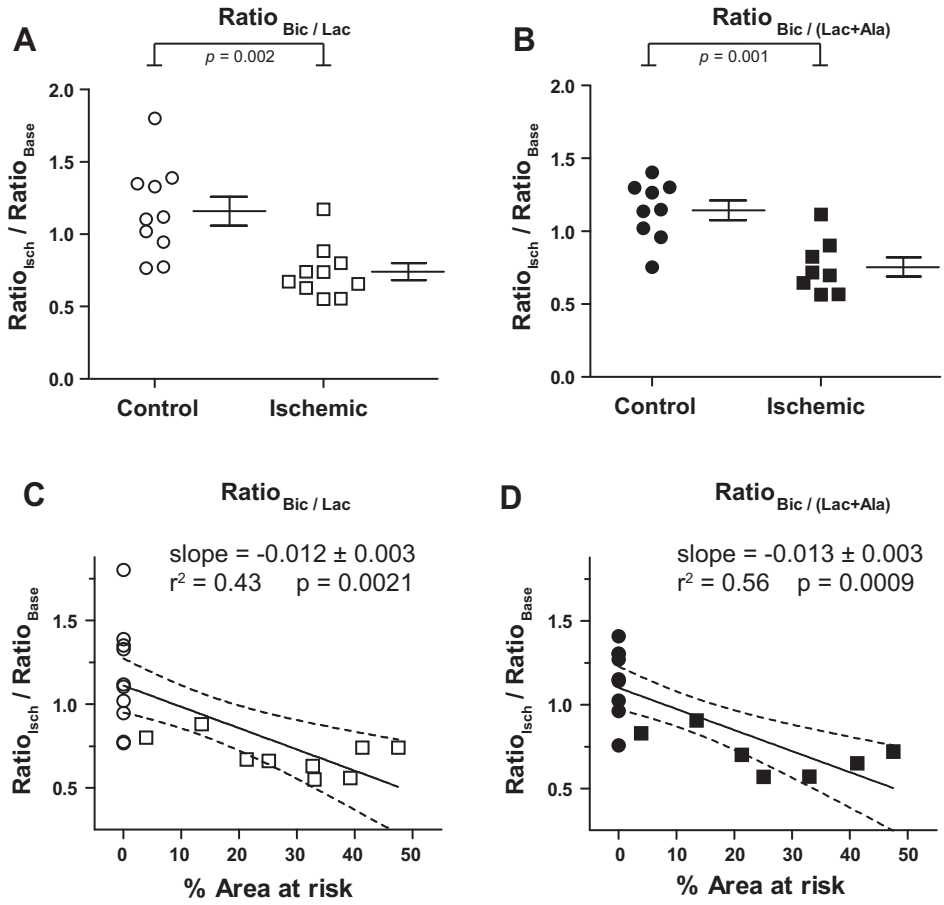

Fig. 3. *A*: changes in conversion of [1-^{13}C]pyruvate to [^{13}C]bicarbonate vs. [1-^{13}C]lactate. Scatter plot of $Ratio_{Isch}/Ratio_{Base}$ using $Ratio_{Bic/Lac}$ for the control (○) and ischemia (□) groups. In the ischemia group, this ratio was lower than in the controls, indicating a shift toward anaerobic metabolism in the myocardium of these animals. In the controls, this ratio was slightly positive, which could be explained by a trend of the myocardium to recover from the initial coronary surgery during the course of the experiment. Horizontal lines and bars indicate means ± SE. *B*: scatter plot of $Ratio_{Isch}/Ratio_{Base}$ for the control (●) and ischemia (■) groups using $Ratio_{Bic/Lac+Ala}$. *C*: scatter plot of $Ratio_{Isch}/Ratio_{Base}$ using $Ratio_{Bic/Lac}$ vs. area at risk. $Ratio_{Isch}/Ratio_{Base}$ correlates with the size of area at risk as determined by Evans blue staining in the ischemia group ($n = 9$). Control experiments (○, $n = 10$) were assigned 0% area at risk. Solid line is the best-fit linear regression with dotted lines showing 95% confidence interval. Slope: −0.014 ± 0.004; *y*-intercept: 1.16 ± 0.08. *D*: scatter plot of $Ratio_{Isch}/Ratio_{Base}$ vs. area at risk using $Ratio_{Bic/Lac+Ala}$. Linear regression slope: −0.013 ± 0.003; *y*-intercept: 1.10 ± 0.06. Ischemia group $n = 7$; control group $n = 9$.

The lower *P* value obtained by using $Ratio_{Bic/Lac+Ala}$ likely results from the smaller range of values in the control group (Fig. 3, *A* and *B*). Similarly, the plot of $Ratio_{Isch}/Ratio_{Base}$ calculated using $Ratio_{Bic/Lac+Ala}$ vs. area at risk (Fig. 3*D*) closely resembles that using $Ratio_{Bic/Lac}$, and the correlation by linear regression approached statistical significance ($P = 0.072$) with the control points excluded.

Alternatively, in looking at the hyperpolarized [^{13}C]bicarbonate and [1-^{13}C]lactate signals relative to [1-^{13}C]alanine, the changes in the lactate-to-alanine and bicarbonate-to-alanine ratios before and after ischemia showed no significant differences. $Ratio_{Isch}/Ratio_{Base}$ calculated using $Ratio_{Lac/Ala}$ was 0.97 ± 0.08 in the ischemia group vs. 0.94 ± 0.14 in controls, whereas the corresponding values for $Ratio_{Bic/Ala}$ (0.75 ± 0.08 and 1.07 ± 0.14, $P = 0.088$) showed the same trend as $Ratio_{Bic/Lac}$.

DISCUSSION

A novel intact small animal model of ischemia-reperfusion is presented, in which the metabolic conversion of infused hyperpolarized [1-^{13}C]pyruvate into [^{13}C]bicarbonate and [1-^{13}C]lactate is quantified by ^{13}C MRS. In the first minutes of reperfusion in this model of LAD ischemia, $Ratio_{Bic/Lac}$ was consistently lower upon reperfusion vs. baseline by ~23%, whereas it did not change in the controls. These findings are consistent with studies on ex vivo perfused heart preparations, which reported increased lactate production and decreased pyruvate dehydrogenase (PDH) activity immediately following a period of global ischemia (28, 38). Although hyperpolarized ^{13}C MRS allows the simultaneous measurement of the pyruvate metabolites bicarbonate, lactate, and alanine, the change in alanine production during early reperfusion was minimal in this model, and, consequently, the integration of the alanine signal did not improve the sensitivity of the method to detect ischemia-reperfusion.

Metabolic alterations during early myocardial reperfusion in the intact small animal model. In the presented model of myocardial ischemia-reperfusion in the intact rat, $Ratio_{Bic/Lac}$ decreased from 0.22 ± 0.09 at baseline to 0.17 ± 0.10 within the first minutes after the release of the coronary artery occlusion as shown in Fig. 2, whereas it did not change in the control group with $Ratio_{Bic/Lac}$ at baseline and during reperfusion of 0.20 ± 0.03 and 0.21 ± 0.02, respectively ($P = 0.017$, 2-way ANOVA with repeated measures). This change in $Ratio_{Bic/Lac}$ was reliably measured in this model of intact rats exposed to a moderate size of ischemic-reperfused myocardium with an area at risk of ~30% of the LV mass. $Ratio_{Bic/Lac}$ decreased by ~23% vs. baseline, which is in agreement with a shift toward anaerobic metabolism in the ischemic region, with a reduction of PDH activity and an increase in the lactate pool. The fact that $Ratio_{Bic/Lac}$ was measured within the first minutes after release of the coronary artery occlusion might be an important factor in the sensitivity to detect a change in metabolism, as bicarbonate production was shown by Merritt and coworkers in a Langendorff heart preparation to recover within minutes upon reperfusion (28). In that study, an AUC of the bicarbon-

ate-to-lactate spectral peak ratio during reperfusion of the entire rat heart of ~0.10 of baseline was reported (Fig. 5 in their publication), translating to a ratio of 0.73 for a heart with a 30% area at risk, which is in line with the value of 0.66 observed in the current study with an area at risk of 28.6 ± 4.7%. The current results suggest that $Ratio_{Bic/Lac}$ can be used in the intact rat model of ischemia-reperfusion to quantify the metabolic changes occurring immediately upon reperfusion. The correlation between the size of the area at risk and the decrease in $Ratio_{Bic/Lac}$ indicates that this technique is probing the metabolism in the ischemic-reperfused myocardium. In this context, it is important to note that no infarcts were produced with this protocol, and thus the myocardium assessed by this technique in principle represents salvageable myocardium. Therefore, this model might be useful to assess novel cardioprotective treatments in an intact animal, thereby testing their impact on metabolism while preserving the neuroendocrine and inflammatory responses activated during reperfusion (35). Such a noninvasive technique to measure metabolism in vivo may therefore also facilitate the translation of animal studies into humans because the presented intact model closely mimics reperfusion of AMI in patients and because clinical studies have been performed using hyperpolarized [1-^{13}C]pyruvate (31).

The metabolite $Ratio_{Bic/Lac}$ to solve the problem of TIF. Besides serving as a sensitive metric for the opposing changes in the conversion of pyruvate to bicarbonate and lactate, $Ratio_{Bic/Lac}$, as suggested by Merritt et al. (28) and later by others (9), can be used to control for changes in perfusion at baseline vs. reperfusion. As both metabolites are produced from a single substrate, i.e., the infused hyperpolarized pyruvate, this metabolite ratio is an elegant means to eliminate the need for a TIF. Supporting this idea, in the current study, the change of $Ratio_{Bic/Lac}$ could differentiate the animals subjected to ischemia-reperfusion from the sham-occluded control animals, and this was achieved by using a relatively small sample size of 20 animals. An alternative approach to directly measure the TIF by imaging would be a demanding task in a small animal model.

Changes in the [1-^{13}C]lactate and [^{13}C]bicarbonate signals reflect the changed metabolic state of the heart. Ischemic myocardium is well known to produce and accumulate lactate (30, 36, 37), as the glycolysis of stored glycogen increases in response to the decreased fuel supply, and NADH accumulates under hypoxic conditions, favoring the reduction of pyruvate to lactate. This change in redox potential has also been detected by the increased NADH fluorescence on the surface of ischemic regions of the heart (11, 32). The rapid interconversion of pyruvate and lactate by lactate dehydrogenase results in the distribution of the labeled hyperpolarized pyruvate into these endogenous metabolite pools, with the observed [1-^{13}C]lactate signal reflecting the tissue lactate levels (24, 45).

The [^{13}C]bicarbonate signal, on the other hand, is due to oxidative decarboxylation of [1-^{13}C]pyruvate by PDH (27) and the pH-dependent equilibration of the resulting $^{13}CO_2$ by carbonic anhydrase (19). The direct relationship between the hyperpolarized [^{13}C]bicarbonate signal and PDH activity has been shown by Atherton (7, 8), Dodd (17, 18), and coworkers, where PDH activity was modulated by diet, disease state, or treatment with thyroid hormone or dichloroacetate. Pyruvate dehydrogenase kinase inhibits PDH by phosphorylation and is in turn regulated by the [NADH]/[NAD^+] and [acetyl-CoA]/[CoA] ratios such that high NADH inhibits PDH activity (23).

The opposing effects of increased NADH levels in ischemic tissue on the oxidation and reduction of [1-^{13}C]pyruvate lead to a lower $Ratio_{Bic/Lac}$ by either or both a decrease in [^{13}C]bicarbonate and an increase in [1-^{13}C]lactate production. In prior rat ex vivo and pig in vivo myocardial ischemia studies using hyperpolarized [1-^{13}C]pyruvate, one or both of these effects have been reported, depending on the model. Ex vivo, Merritt et al. (28) note both a dramatic increase in lactate and decrease in bicarbonate signal in early reperfusion, whereas Ball et al. (9) note an increase in lactate (normalized to pyruvate signal) in the ischemic region. In pigs, Golman and coworkers observed a 41 ± 7.8% reduction in bicarbonate signal in stunned myocardium after 2 h of reperfusion, with a variable but insignificant change in lactate (21). Similarly, in pigs, Lau and coworkers (25) reported a significant reduction in pyruvate-normalized bicarbonate signal in the anterior wall of the LV 45 min after a 60-min period of anterior ischemia along with an increase in normalized lactate. More recently in another pig model, Aquaro and coworkers (4) reported a significant increase in lactate signal and a significant decrease of bicarbonate signal comparing affected and unaffected regions 5 min following 10 min of LAD occlusion.

While each of these prior studies used different experimental protocols and data acquisition methods, the common metabolic changes of decreased bicarbonate signal and/or increased lactate further support the idea that $Ratio_{Bic/Lac}$ is an appropriate and likely more sensitive metric of the metabolic state of postischemic tissue than either metabolite alone. Among the studies using hyperpolarized ^{13}C MRS to follow metabolism in ischemic-reperfused myocardium in vivo, the current study is notably the first performed in intact rats, as well as the first to apply the $Ratio_{Bic/Lac}$ metric in vivo. This study also shows that coil-localized MRS is sufficient to detect metabolic changes in such a model, and it probes energy metabolism immediately upon reperfusion, i.e., at an earlier stage of reperfusion than previous in vivo studies.

The alanine signal does not contribute to characterization of ischemia-reperfusion. Hyperpolarized [1-^{13}C]alanine was also considered as a potential metabolic marker because alanine levels have been reported by Peuhkurinen and coworkers (36) to increase twofold in the rat heart after 10 min of global ischemia, and Pisarenko and coworkers (37) reported a three- to fourfold increase in the guinea pig heart after 15 min of global hypoperfusion (37). On the other hand, in a large animal model of localized ischemia, Golman and coworkers (21) reported a 5.8% decrease of hyperpolarized alanine signal in the diseased area in pigs following 15 min of ischemia and a decrease of 56% after 45 min of ischemia (21). In the current model of localized ischemia, [1-^{13}C]alanine peaks could be quantitated in all but three experiments, but no significant changes (vs. controls) were observed for [1-^{13}C]alanine, which was on average 6% higher in the ischemia group (Fig. 4). By comparison, [^{13}C]bicarbonate was 20% lower, and [1-^{13}C]lactate 24% higher in the ischemia than in controls. This finding is in line with the aforementioned experiments of Peuhkurinen and Pisarenko, which found lactate to increase during no-flow and low-flow ischemia by more than 12-fold, whereas alanine increased by up to 4.6-fold. Considering the relatively modest increase of 20% observed for the hyperpolarized [1-^{13}C]lactate

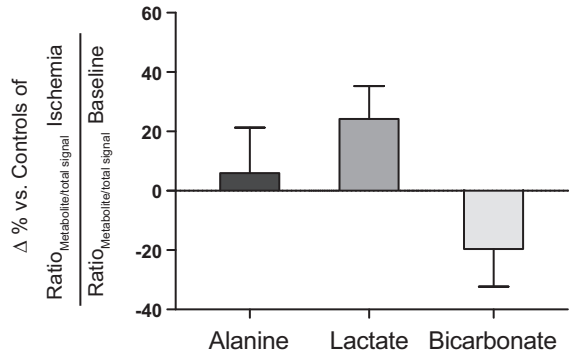

Fig. 4. Changes in pyruvate metabolism from baseline to ischemia. The means of [$Ratio_{Metabolite/total\ signal(Ischemia)}$/$Ratio_{Metabolite/total\ signal(Baseline)}$] are plotted as the percentage difference from the control values for each of [1-^{13}C]alanine, [1-^{13}C]lactate, and [^{13}C]bicarbonate. Compared with the control group, small changes for alanine were observed for the ischemia group. Conversion to lactate tended to increase in the ischemic groups, whereas a decrease was observed for bicarbonate, consistent with a shift to anaerobic metabolism.

signal in the current study, one would expect the correspondingly smaller changes in [1-^{13}C]alanine. A recent study by Chouchani and coworkers (15) also notes small changes in heart alanine levels during ischemia. In ex vivo heart preparations with global ischemia, they found a greater than twofold increase in alanine using liquid chromatography-mass spectrometry. However, no increase in alanine was observed by Chouchani and coworkers in localized myocardial ischemia induced by LAD occlusion in intact mice. These findings illustrate the importance of testing metabolism in various ex vivo but also in in vivo intact animal models.

From a diagnostic point of view, adding data on alanine to the $Ratio_{Bic/Lac}$ did not substantially improve the sensitivity of our experiments to detect differences between control and ischemia-reperfusion animals. Conversely, the similar trend between $Ratio_{Bic/Ala}$ and $Ratio_{Bic/Lac}$, as well as the minimal changes in $Ratio_{Lac/Ala}$, indicate that, as expected, alanine and lactate levels both change in the same direction during ischemia-reperfusion.

Limitations. Surface-coil localized pulse-acquire spectroscopy has the advantage in dynamic hyperpolarized experiments of being technically uncomplicated and offering the highest sensitivity, which is an important consideration for measuring lower-intensity metabolite signals such as [^{13}C]bicarbonate. However, this spectroscopic approach comes at the expense of the spatial information that imaging experiments provide. Given that the ischemic area was in the anterior wall of the LV, it was well placed within the most sensitive region of the coil. Nonetheless, the acquired spectra integrate, not only signals from the myocardium, but also those from the blood in the ventricles, the atria, vasculature, and even parts of the lungs. Hyperpolarized metabolites observed in the liver, such as [1-^{13}C]aspartate and [1-^{13}C]malate, were not detected, indicating no contaminating liver signal. It was assumed that the contribution of hyperpolarized metabolite signals from the blood was comparable for baseline and reperfusion conditions. In fact, in our experiments, no significant change in the blood lactate levels was observed after 10 min of ischemia vs. baseline. Furthermore, the coil position was kept unchanged between the baseline and reperfusion acquisitions, so any extraneous signals would be largely constant throughout the experiment.

The postoperative, physiologically weakened state of the rats is a significant limitation of this open-chest model of myocardial ischemia-reperfusion. A recently described closed-chest model of myocardial ischemia-reperfusion in rats using an implanted balloon occluder (33) offers an attractive alternative that would appear to overcome many of the limitations of open-chest models.

The ratiometric approach of hyperpolarized signals presented in this study avoids the need to determine a tissue input function and provides useful quantitative but relative metabolic measurements. While the lactate pool size and PDH flux have the greatest influence on the conversion of pyruvate to lactate and bicarbonate, other factors such as fatty acid oxidation can have a marked effect (10, 27, 29). To minimize these influences, all animals were studied in the fed state at the same time of day.

Finally, the area at risk was used as a rough surrogate for the mass of ischemic-reperfused myocardium. Microsphere injections would yield more precise measures of hypoperfusion within the area at risk but were deemed too challenging to perform within the magnet.

Conclusions. An intact small animal model of ischemia-reperfusion is presented, which allows for the noninvasive, near real-time assessment of metabolic alterations that occur immediately upon myocardial reperfusion. The $Ratio_{Bic/Lac}$ discriminates ischemic-reperfused from normal myocardium without the need to determine an input function at the tissue level. Information on alanine production does not substantially improve the sensitivity of the technique to detect metabolic alterations immediately upon reperfusion in this intact small animal model. This study establishes the model as a useful complement to ex vivo heart preparations and represents a promising platform to investigate reperfusion metabolism noninvasively in an intact animal, thereby preserving activated neuroendocrine axis and inflammation processes. In the setting of translational research, this model may also be most useful to evaluate novel treatment strategies targeted to reduce reperfusion injury of the heart.

ACKNOWLEDGMENTS

We thank Carola Romero, Mario Lepore, Anne-Catherine Clerc, and Corina Berset for invaluable assistance with the animal experiments and Najat Salameh for administrative support.

Current affiliation for J. Bastiaansen: Department of Radiology, Lausanne University Hospital (CHUV) and University of Lausanne (UNIL), Lausanne, Switzerland.

GRANTS

This work was supported by Swiss National Science Foundation grants no. 310030_138146 and PPOOP1_133562.

DISCLOSURES

No conflicts of interest, financial or otherwise, are declared by the authors.

AUTHOR CONTRIBUTIONS

Author contributions: H.A.Y., J.A.B., and C.B. performed experiments; H.A.Y., J.A.B., C.B., and J.S. analyzed data; H.A.Y., C.B., and J.S. interpreted results of experiments; H.A.Y. and J.S. prepared figures; H.A.Y. and J.S. drafted manuscript; H.A.Y., J.A.B., A.C., and J.S. edited and revised manuscript; H.A.Y., J.A.B., C.B., A.C., and J.S. approved final version of manuscript; A.C. and J.S. conception and design of research.

REFERENCES

1. *Global Health Risks*. Geneva, Switzerland: World Health Organization, 2009, p. 62.
2. **Akki A, Gupta A, Weiss RG.** Magnetic resonance imaging and spectroscopy of the murine cardiovascular system. *Am J Physiol Heart Circ Physiol* 304: H633–H648, 2013.
3. **Aquaro GD, Frijia F, Positano V, Menichetti L, Santarelli MF, Ardenkjaer-Larsen JH, Wiesinger F, Lionetti V, Romano SL, Bianchi G, Neglia D, Giovannetti G, Schulte RF, Recchia FA, Landini L, Lombardi M.** 3D CMR mapping of metabolism by hyperpolarized 13C-pyruvate in ischemia-reperfusion. *JACC Cardiovasc Imaging* 6: 743–744, 2013.
4. **Aquaro GD, Frijia F, Positano V, Menichetti L, Santarelli MF, Lionetti V, Giovannetti G, Recchia FA, Landini L.** Cardiac metabolism in a pig model of ischemia-reperfusion by cardiac magnetic resonance with hyperpolarized 13C-pyruvate. *IJC Metab Endocr* 6: 17–23, 2015.
5. **Atar D, Arheden H, Berdeaux A, Bonnet JL, Carlsson M, Clemmensen P, Cuvier V, Danchin N, Dubois-Rande JL, Engblom H, Erlinge D, Firat H, Halvorsen S, Hansen HS, Hauke W, Heiberg E, Koul S, Larsen AI, Le Corvoisier P, Nordrehaug JE, Paganelli F, Pruss RM, Rousseau H, Schaller S, Sonou G, Tuseth V, Veys J, Vicaut E, Jensen SE.** Effect of intravenous TRO40303 as an adjunct to primary percutaneous coronary intervention for acute ST-elevation myocardial infarction: MITOCARE study results. *Eur Heart J* 36: 112–119, 2015.
6. **Atar D, Petzelbauer P, Schwitter J, Huber K, Rensing B, Kasprzak JD, Butter C, Grip L, Hansen PR, Süselbeck T, Clemmensen PM, Marin-Galiano M, Geudelin B, Buser PT; F.I.R.E. Investigators.** Effect of intravenous FX06 as an adjunct to primary percutaneous coronary intervention for acute ST-segment elevation myocardial infarction results of the F.I.R.E. (Efficacy of FX06 in the Prevention of Myocardial Reperfusion Injury) trial. *J Am Coll Cardiol* 53: 720–729, 2009.
7. **Atherton HJ, Dodd MS, Heather LC, Schroeder MA, Griffin JL, Radda GK, Clarke K, Tyler DJ.** Role of pyruvate dehydrogenase inhibition in the development of hypertrophy in the hyperthyroid rat heart: a combined magnetic resonance imaging and hyperpolarized magnetic resonance spectroscopy study. *Circulation* 123: 2552–2561, 2011.
8. **Atherton HJ, Schroeder MA, Dodd MS, Heather LC, Carter EE, Cochlin LE, Nagel S, Sibson NR, Radda GK, Clarke K, Tyler DJ.** Validation of the in vivo assessment of pyruvate dehydrogenase activity using hyperpolarised 13C MRS. *NMR Biomed* 24: 201–208, 2011.
9. **Ball DR, Cruickshank R, Carr CA, Stuckey DJ, Lee P, Clarke K, Tyler DJ.** Metabolic imaging of acute and chronic infarction in the perfused rat heart using hyperpolarised [1-13C]pyruvate. *NMR Biomed* 26: 1441–1450, 2013.
10. **Ball DR, Rowlands B, Dodd MS, Le Page L, Ball V, Carr CA, Clarke K, Tyler DJ.** Hyperpolarized butyrate: a metabolic probe of short chain fatty acid metabolism in the heart. *Magn Reson Med* 71: 1663–1669, 2014.
11. **Barlow CH, Chance B.** Ischemic areas in perfused rat hearts: measurement by NADH fluorescence photography. *Science* 193: 909–910, 1976.
12. **Chapon C, Herlihy AH, Bhakoo KK.** Assessment of myocardial infarction in mice by late gadolinium enhancement MR imaging using an inversion recovery pulse sequence at 9.4T. *J Cardiovasc Magn Reson* 10: 6, 2008.
13. **Cheng T, Capozzi A, Takado Y, Balzan R, Comment A.** Over 35% liquid-state 13C polarization obtained via dissolution dynamic nuclear polarization at 7 T and 1 K using ubiquitous nitroxyl radicals. *Phys Chem Chem Phys* 15: 20819–20822, 2013.
14. **Cheng T, Mishkovsky M, Bastiaansen JAM, Ouari O, Hautle P, Tordo P, van den Brandt B, Comment A.** Automated transfer and injection of hyperpolarized molecules with polarization measurement prior to in vivo NMR. *NMR Biomed* 26: 1582–1588, 2013.
15. **Chouchani ET, Pell VR, Gaude E, Aksentijevic D, Sundier SY, Robb EL, Logan A, Nadtochiy SM, Ord ENJ, Smith AC, Eyassu F, Shirley R, Hu CH, Dare AJ, James AM, Rogatti S, Hartley RC, Eaton S, Costa ASH, Brookes PS, Davidson SM, Duchen MR, Saeb-Parsy K, Shattock MJ, Robinson AJ, Work LM, Frezza C, Krieg T, Murphy MP.** Ischaemic accumulation of succinate controls reperfusion injury through mitochondrial ROS. *Nature* 515: 431–435, 2014.
16. **Comment A, van den Brandt B, Uffmann K, Kurdzesau F, Jannin S, Konter JA, Hautle P, Wenckebach WT, Gruetter R, van der Klink JJ.** Design and performance of a DNP prepolarizer coupled to a rodent MRI scanner. *Concepts Magn Reson B Magn Reson Eng* 31B: 255–269, 2007.
17. **Dodd MS, Atherton HJ, Carr CA, Stuckey DJ, West JA, Griffin JL, Radda GK, Clarke K, Heather LC, Tyler DJ.** Impaired in vivo mitochondrial Krebs cycle activity after myocardial infarction assessed using hyperpolarized magnetic resonance spectroscopy. *Circ Cardiovasc Imaging* 7: 895–904, 2014.
18. **Dodd MS, Ball DR, Schroeder MA, Le Page LM, Atherton HJ, Heather LC, Seymour AM, Ashrafian H, Watkins H, Clarke K, Tyler DJ.** In vivo alterations in cardiac metabolism and function in the spontaneously hypertensive rat heart. *Cardiovasc Res* 95: 69–76, 2012.
19. **Gallagher FA, Kettunen MI, Day SE, Hu DE, Ardenkjaer-Larsen JH, Zandt R, Jensen PR, Karlsson M, Golman K, Lerche MH, Brindle KM.** Magnetic resonance imaging of pH in vivo using hyperpolarized 13C-labelled bicarbonate. *Nature* 453: 940–943, 2008.
20. **Golman K, in 't Zandt R, Thaning M.** Real-time metabolic imaging. *Proc Natl Acad Sci USA* 103: 11270–11275, 2006.
21. **Golman K, Petersson JS, Magnusson P, Johansson E, Akeson P, Chai CM, Hansson G, Mansson S.** Cardiac metabolism measured noninvasively by hyperpolarized 13C MRI. *Magn Reson Med* 59: 1005–1013, 2008.
22. **Gruetter R, Tkac I.** Field mapping without reference scan using asymmetric echo-planar techniques. *Magn Reson Med* 43: 319–323, 2000.
23. **Kerbey AL, Randle PJ, Cooper RH, Whitehouse S, Pask HT, Denton RM.** Regulation of pyruvate dehydrogenase in rat heart. Mechanism of regulation of proportions of dephosphorylated and phosphorylated enzyme by oxidation of fatty acids and ketone bodies and of effects of diabetes: role of coenzyme A, acetyl-coenzyme A and reduced and oxidized nicotinamide-adenine dinucleotide. *Biochem J* 154: 327–348, 1976.
24. **Kettunen MI, Hu DE, Witney TH, McLaughlin R, Gallagher FA, Bohndiek SE, Day SE, Brindle KM.** Magnetization transfer measurements of exchange between hyperpolarized [1-13C]pyruvate and [1-13C]lactate in a murine lymphoma. *Magn Reson Med* 63: 872–880, 2010.
25. **Lau AZ, Chen AP, Barry J, Graham JJ, Dominguez-Viqueira W, Ghugre NR, Wright GA, Cunningham CH.** Reproducibility study for free-breathing measurements of pyruvate metabolism using hyperpolarized C-13 in the heart. *Magn Reson Med* 69: 1063–1071, 2013.
26. **Luft D, Deichsel G, Schmülling RM, Stein W, Eggstein M.** Definition of clinically relevant lactic acidosis in patients with internal diseases. *Am J Clin Pathol* 80: 484–489, 1983.
27. **Merritt ME, Harrison C, Storey C, Jeffrey FM, Sherry AD, Malloy CR.** Hyperpolarized 13C allows a direct measure of flux through a single enzyme-catalyzed step by NMR. *Proc Natl Acad Sci USA* 104: 19773–19777, 2007.
28. **Merritt ME, Harrison C, Storey C, Sherry AD, Malloy CR.** Inhibition of carbohydrate oxidation during the first minute of reperfusion after brief ischemia: NMR detection of hyperpolarized 13CO2 and H13CO3. *Magn Reson Med* 60: 1029–1036, 2008.
29. **Moreno KX, Sabelhaus SM, Merritt ME, Sherry AD, Malloy CR.** Competition of pyruvate with physiological substrates for oxidation by the heart: implications for studies with hyperpolarized [1-13C]pyruvate. *Am J Physiol Heart Circ Physiol* 298: H1556–H1564, 2010.
30. **Neely JR, Rovetto MJ, Whitmer JT, Morgan HE.** Effects of ischemia on function and metabolism of the isolated working rat heart. *Am J Physiol* 225: 651–658, 1973.
31. **Nelson SJ, Kurhanewicz J, Vigneron DB, Larson PEZ, Harzstark AL, Ferrone M, Van Criekinge M, Chang JW, Bok R, Park I, Reed G, Carvajal L, Small EJ, Munster P, Weinberg VK, Ardenkjaer-Larsen JH, Chen AP, Hurd RE, Odegardstuen LI, Robb FJ, Tropp J, Murray JA.** Metabolic imaging of patients with prostate cancer using hyperpolarized [1-13C]pyruvate. *Sci Transl Med* 5: 198ra108, 2013.
32. **Nuutinen EM.** Subcellular origin of the surface fluorescence of reduced nicotinamide nucleotides in the isolated perfused rat heart. *Basic Res Cardiol* 79: 49–58, 1984.
33. **h-Ici DO, Jeuthe S, Dietrich T, Berger F, Kuehne T, Kozerke S, Messroghli DR.** Closed-chest small animal model to study myocardial infarction in an MRI environment in real time. *Int J Cardiovasc Imaging* 31: 115–121, 2015.
34. **O'Gara PT, Kushner FG, Ascheim DD, Casey DE, Chung MK, de Lemos JA, Ettinger SM, Fang JC, Fesmire FM, Franklin BA, Granger CB, Krumholz HM, Linderbaum JA, Morrow DA, Newby LK, Ornato JP, Ou N, Radford MJ, Tamis-Holland JE, Tommaso CL, Tracy CM, Woo YJ, Zhao DX, Anderson JL, Jacobs AK, Halperin JL, Albert NM, Brindis RG, Creager MA, DeMets D, Guyton RA, Hochman JS, Kovacs RJ, Kushner FG, Ohman EM, Stevenson WG, Yancy CW; American College of Emergency Physicians; Society for Cardio-**

vascular Angiography and Interventions. 2013 ACCF/AHA guideline for the management of ST-elevation myocardial infarction: a report of the American College of Cardiology Foundation/American Heart Association Task Force on Practice Guidelines. *J Am Coll Cardiol* 61: e78–e140, 2013.

35. **Oliver MF, Opie LH.** Effects of glucose and fatty acids on myocardial ischaemia and arrhythmias. *Lancet* 343: 155–158, 1994.
36. **Peuhkurinen KJ, Takala TE, Nuutinen EM, Hassinen IE.** Tricarboxylic acid cycle metabolites during ischemia in isolated perfused rat heart. *Am J Physiol Heart Circ Physiol* 244: H281–H288, 1983.
37. **Pisarenko OI, Studneva IM, Shulzhenko VS, Kapelko VI.** Relations between the energy state of the myocardium and release of some products of anaerobic metabolism during underperfusion. *Pflügers Arch* 416: 434–441, 1990.
38. **Schroeder MA, Atherton HJ, Ball DR, Cole MA, Heather LC, Griffin JL, Clarke K, Radda GK, Tyler DJ.** Real-time assessment of Krebs cycle metabolism using hyperpolarized 13C magnetic resonance spectroscopy. *FASEB J* 23: 2529–2538, 2009.
39. **Schroeder MA, Atherton HJ, Dodd MS, Lee P, Cochlin LE, Radda GK, Clarke K, Tyler DJ.** The cycling of acetyl-coenzyme A through acetylcarnitine buffers cardiac substrate supply: a hyperpolarized 13C magnetic resonance study. *Circ Cardiovasc Imaging* 5: 201–209, 2012.
40. **Schroeder MA, Cochlin LE, Heather LC, Clarke K, Radda GK, Tyler DJ.** In vivo assessment of pyruvate dehydrogenase flux in the heart using hyperpolarized carbon-13 magnetic resonance. *Proc Natl Acad Sci USA* 105: 12051–12056, 2008.
41. **Schroeder MA, Swietach P, Atherton HJ, Gallagher FA, Lee P, Radda GK, Clarke K, Tyler DJ.** Measuring intracellular pH in the heart using hyperpolarized carbon dioxide and bicarbonate: a 13C and 31P magnetic resonance spectroscopy study. *Cardiovasc Res* 86: 82–91, 2010.
42. **Selker HP, Beshansky JR, Sheehan PR, Massaro JM, Griffith JL, D'Agostino RB, Ruthazer R, Atkins JM, Sayah AJ, Levy MK, Richards ME, Aufderheide TP, Braude DA, Pirrallo RG, Doyle DD, Frascone RJ, Kosiak DJ, Leaming JM, Van Gelder CM, Walter GP, Wayne MA, Woolard RH, Opie LH, Rackley CE, Apstein CS, Udelson JE.** Out-of-hospital administration of intravenous glucose-insulin-potassium in patients with suspected acute coronary syndromes: the IMMEDIATE randomized controlled trial. *J Am Med Soc* 307: 1925–1933, 2012.
43. **Seymour AM, Giles L, Ball V, Miller JJ, Clarke K, Carr CA, Tyler DJ.** In vivo assessment of cardiac metabolism and function in the abdominal aortic banding model of compensated cardiac hypertrophy. *Cardiovasc Res* 106: 249–260, 2015.
44. **Windecker S, Kolh P, Alfonso F, Collet JP, Cremer J, Falk V, Filippatos G, Hamm C, Head SJ, Jüni P, Kappetein AP, Kastrati A, Knuuti J, Landmesser U, Laufer G, Neumann FJ, Richter DJ, Schauerte P, Sousa Uva M, Stefanini GG, Taggart DP, Torracca L, Valgimigli M, Wijns W, Witkowski A.** 2014 ESC/EACTS Guidelines on myocardial revascularization: The Task Force on Myocardial Revascularization of the European Society of Cardiology (ESC) and the European Association for Cardio-Thoracic Surgery (EACTS). Developed with the special contribution of the European Association of Percutaneous Cardiovascular Interventions (EAPCI). *Eur Heart J* 35: 2541–2619, 2014.
45. **Witney TH, Kettunen MI, Brindle KM.** Kinetic modeling of hyperpolarized 13C label exchange between pyruvate and lactate in tumor cells. *J Biol Chem* 286: 24572–24580, 2011.
46. **Yellon DM, Hausenloy DJ.** Myocardial reperfusion injury. *N Engl J Med* 357: 1121–1135, 2007.